THE ROYAL SOCIETY

Revealing a lognormal cascading process in turbulent velocity statistics with wavelet analysis

By A. Arneodo[1], S. Manneville[2], J. F. Muzy[1] and S. G. Roux[3]

[1]*Centre de Recherche Paul Pascal, Avenue Schweitzer, 33600, Pessac, France*
[2]*Laboratoire Ondes et Acoustique, ESPCI, 10 rue Vauquelin, 75005 Paris, France*
[3]*NASA Goddard Space Flight Center, Climate and Radiation Branch (Code 913), Greenbelt, MD 20771, USA*

We use the continuous wavelet transform to extract a cascading process from experimental turbulent velocity signals. We mainly investigate various statistical quantities such as the singularity spectrum, the self-similarity kernel and space-scale correlation functions, which together provide information about the possible existence and nature of the underlying multiplicative structure. We show that, at the highest accessible Reynolds numbers, the experimental data do not allow us to distinguish various phenomenological cascade models recently proposed to account for intermittency from their lognormal approximation. In addition, we report evidence that velocity fluctuations are not scale-invariant but possess more complex self-similarity properties, which are likely to depend on the Reynolds number. We comment on the possible asymptotic validity of the multifractal description.

Keywords: turbulence; wavelet analysis; intermittency; self-similarity; cascade models; multifractals

1. Introduction

Since Kolmogorov's founding work (Kolmogorov 1941) (hereafter called K41), fully developed turbulence has been intensively studied for more than 50 years (Monin & Yaglom 1975; Frisch & Orzag 1990; Frisch 1995). A standard way of analysing a turbulent flow is to look for some universal statistical properties of the fluctuations of the longitudinal velocity increments over a distance l, $\delta v_l = v(x+l) - v(x)$. For instance, investigating the scaling properties of the structure functions,

$$S_p(l) = \langle |\delta v_l|^p \rangle \sim l^{\zeta_p}, \quad p > 0, \tag{1.1}$$

where $\langle \cdots \rangle$ stands for ensemble average, leads to a spectrum of scaling exponents ζ_p, which has been widely used as a statistical characterization of turbulent fields (Monin & Yaglom 1975; Frisch & Orzag 1990; Frisch 1995). Based upon assumptions of statistical homogeneity, isotropy and of constant rate ϵ of energy transfer from large to small scales, K41 theory predicts the existence of an inertial range $\eta \ll l \ll L$ (η and L being, respectively, the dissipative and integral scales), where $S_p(l) \sim \epsilon^{p/3} l^{p/3}$. Although these assumptions are usually considered to be correct, there has been increasing numerical (Briscolini *et al.* 1994; Vincent & Meneguzzi 1995) and

experimental (Monin & Yaglom 1975; Anselmet *et al.* 1984; Gagne 1987; Frisch & Orzag 1990; Frisch 1995; Tabeling & Cardoso 1995; Arneodo *et al.* 1996) evidence that ζ_p deviates substantially from the K41 prediction $\zeta_p = \frac{1}{3}p$, at large p. The observed nonlinear behaviour of ζ_p is generally interpreted as a direct consequence of the intermittency phenomenon displayed by the rate of energy transfer (Castaing *et al.* 1990; Meneveau & Sreenivasan 1991). Under the so-called Kolmogorov's refined hypothesis (Kolmogorov 1962), the velocity structure functions can be rewritten as

$$S_p(l) \sim \langle \epsilon_l^{p/3} \rangle l^{p/3} \sim l^{\tau(p/3)+p/3},$$

where ϵ_l is the local rate of energy transfer over a volume of size l. The scaling exponents of S_p are thus related to those of the energy transfer: $\zeta_p = \tau(\frac{1}{3}p) + \frac{1}{3}p$.

Richardson's (1926) cascade pioneering picture is often invoked to account for intermittency: energy is transferred from large eddies (of size of order L) down to small scales (of order η) through a cascade process in which the transfer rate at a given scale is not spatially homogeneous as in the K41 theory but undergoes local intermittent fluctuations. Over the past 30 years, refined models—including the log-normal model of Kolmogorov (1962) and Obukhov (1962) (hereafter called KO62), multiplicative hierarchical cascade models, such as the random β-model, the α-model, the p-model (for a review see Meneveau & Sreenivasan (1991)), the log-stable models (Schertzer & Levejoy 1987; Kida 1990), and more recently the log-infinitely divisible cascade models (Novikov 1990, 1995; Dubrulle 1994; She & Waymire 1995; Castaing & Dubrulle 1995), together with the rather popular log-Poisson model advocated by She & Leveque (1994)—have appeared in the literature as reasonable models for mimicking the energy cascading process in turbulent flows. Unfortunately, all the existing models appeal to adjustable parameters that are difficult to determine by plausible physical arguments and that generally provide enough freedom to account for the experimental data for the two sets of scaling exponents ζ_p and $\tau(p)$.

The scaling behaviour of the velocity structure functions (equation (1.1)) is at the heart of the multifractal description pioneered by Parisi & Frisch (1985). K41 theory is actually based on the assumption that at each point of the fluid the velocity field has the same scaling behaviour $\delta v_l(x) \sim l^{1/3}$, which yields the well-known $E(k) \sim k^{-5/3}$ energy spectrum. By interpreting the nonlinear behaviour of ζ_p as a direct consequence of the existence of spatial fluctuations in the local regularity of the velocity field, $\delta v_l(x) \sim l^{h(x)}$, Parisi & Frisch (1985) attempt to capture intermittency in a geometrical framework. For each h, let us call $D(h)$ the fractal dimension of the set for which $\delta v_l(x) \sim l^h$. By suitably inserting this local scaling behaviour into equation (1.1), one can bridge the so-called singularity spectrum $D(h)$ and the set of scaling exponents ζ_p by a Legendre transform: $D(h) = \min_p(ph - \zeta_p + 1)$. From the properties of the Legendre transform, a nonlinear ζ_p spectrum is equivalent to the assumption that there is more than a single scaling exponent h. Let us note that from low- to moderate-Reynolds-number turbulence, the inertial scaling range is small and the evaluation of ζ_p is not very accurate. Actually, the existence of scaling laws like equation (1.1) for the structure functions is not clear experimentally (Arneodo *et al.* 1996; Pedrizetti *et al.* 1996), even at the highest accessible Reynolds numbers; this observation questions the validity of the multifractal description. Recently, Benzi *et al.* (1993*b*, *c*, 1995) have shown that one can remedy the observed departure from scale-invariance by looking at the scaling behaviour of one structure function against another. More precisely, ζ_p can be estimated from the behaviour $S_p(l) \sim S_3(l)^{\zeta_p}$, if

one assumes that $\zeta(3) = 1$ (Frisch 1995). The relevance of the so-called extended self-similarity (ESS) hypothesis is recognized to improve and to further extend the scaling behaviour towards the dissipative range (Benzi *et al.* 1993*b*, *c*, 1995; Briscolini *et al.* 1994). From the application of ESS, some experimental consensus has been reached on the definite nonlinear behaviour of ζ_p and its possible universal character, at least as far as isotropic homogeneous turbulence is concerned (Arneodo *et al.* 1996). But beyond some practical difficulties there exists a more fundamental insufficiency in the determination of ζ_p. From the analogy between the multifractal formalism and statistical thermodynamics (Arneodo *et al.* 1995), ζ_p plays the role of a thermodynamical potential which intrinsically contains only some degenerate information about the 'Hamiltonian' of the problem, i.e. the underlying cascading process. Therefore, it is not surprising that previous experimental determinations of the ζ_p spectrum have failed to provide a selective test to discriminate between various (deterministic or random) cascade models.

In order to go beyond the multifractal description, Castaing and co-workers (Castaing *et al.* 1990, 1993; Gagne *et al.* 1994; Naert *et al.* 1994; Chabaud *et al.* 1994; Castaing & Dubrulle 1995; Chillà *et al.* 1996) have proposed an intermittency phenomenon approach which relies on the validity of Kolmogorov's refined hypothesis (Kolmogorov 1962) and which consists in looking for a multiplicative cascade process directly on the velocity field. This approach amounts to modelling the evolution of the shape of the velocity increment probability distribution function (PDF), from Gaussian at large scales to more intermittent profiles with stretched exponential-like tails at smaller scales (Gagne 1987; Castaing *et al.* 1990; Kailasnath *et al.* 1992; Tabeling *et al.* 1996; Belin *et al.* 1996), by a functional equation that relates the two scales using a kernel G. This description relies upon the ansatz that the velocity increment PDF at a given scale l, $P_l(\delta v)$, can be expressed as a weighted sum of dilated PDFs at a larger scale $l' > l$:

$$P_l(\delta v) = \int G_{ll'}(\ln \sigma) \frac{1}{\sigma} P_{l'}\left(\frac{\delta v}{\sigma}\right) \mathrm{d} \ln \sigma, \tag{1.2}$$

where $G_{ll'}$ is a kernel that depends on l and l' only. Indeed, most of the well-known cascade models can be reformulated within this approach (Castaing & Dubrulle 1995; Chillà *et al.* 1996). This amounts to (i) specifying the shape of the kernel $G(u)$ which is determined by the nature of the elementary step in the cascade; and (ii) defining the way $G_{ll'}$ depends on both l and l'. In their original work, Castaing *et al.* (see Castaing *et al.* 1990, 1993; Gagne *et al.* 1994; Naert *et al.* 1994; Chabaud *et al.* 1994) mainly focused on the estimate of the variance of G and its scale behaviour. A generalization of the Castaing *et al.* ansatz to the wavelet transform (WT) of the velocity field has been proposed in previous works (Arneodo *et al.* 1997, 1999; Roux 1996) and shown to provide direct access to the entire shape of the kernel G. This wavelet-based method has been tested on synthetic turbulent signals and preliminarily applied to turbulence data. In § 2, we use this new method to process large-velocity records in high-Reynolds-number turbulence (Arneodo *et al.* 1998*c*). We start by briefly recalling our numerical method to estimate G. We then focus on the precise shape of G and show that, for the analysed turbulent flows, G is Gaussian within a very good approximation. Special attention is paid to statistical convergence; in particular, we show that when exploring larger samples than in previous studies (Arneodo *et al.* 1997, 1999; Roux 1996), one is able to discriminate between lognormal

and log-Poisson statistics. However, in the same way the ζ_p and $D(h)$ multifractal spectra provide rather degenerate information about the nature of the underlying process; equation (1.2) is a necessary but not sufficient condition for the existence of a cascade. As emphasized in a recent work (Arneodo *et al.* 1998*a*), one can go deeper in fractal analysis by studying correlation functions in both space and scales using the continuous wavelet transform. This 'two-point' statistical analysis has proved to be particularly well suited for studying multiplicative random cascade processes for which the correlation functions take a very simple form. In § 3, we apply space-scale correlation functions to high-Reynolds-number turbulent velocity signals. This method confirms the existence of a cascade structure that extends over the inertial range and that this cascade is definitely not scale-invariant. In § 4, we revisit the multifractal description of turbulent velocity fluctuations under the objective of the WT microscope. Going back to the WT coefficient PDFs and to the ζ_p spectrum, we get additional confirmation of the relevance of a lognormal cascading process. Furthermore, we discuss its robustness when varying the scale range or the Reynolds number. We conclude in § 5 by discussing the asymptotic validity of the multifractal description of the intermittency phenomenon in fully developed turbulence.

Throughout this study, we will compare the results obtained on experimental data with the results of similar statistical analysis of lognormal and log-Poisson numerical processes of the same length generated using an algorithm of multiplicative cascade defined on an orthonormal wavelet basis. We refer the reader to Roux (1996), Arneodo *et al.* (1997, 1998*b*, *c*, 1999) and § 3 *b*, where the main points of this synthetic turbulence generator are described.

2. Experimental evidence for lognormal statistics in high-Reynolds-number turbulent flows

(*a*) *A method for determining the kernel G*

As pointed out in Muzy *et al.* (1991, 1994) and Arneodo *et al.* (1995), the WT provides a powerful mathematical framework for analysing irregular signals in both space and scale without loss of information. The WT of the turbulent velocity spatial field v at point x and scale $a > 0$, is defined as (Meyer 1990; Daubechies 1992)

$$T_\psi[v](x,a) = \frac{1}{a}\int_{-\infty}^{+\infty} v(y)\psi\left(\frac{x-y}{a}\right)\mathrm{d}y, \tag{2.1}$$

where ψ is the analysing wavelet. Note that the velocity increment $\delta v_l(x)$ is simply $T_\psi[v](x,l)$ computed with the 'poor man's' wavelet

$$\psi^{(1)}_{(0)}(x) = \delta(x-1) - \delta(x).$$

More generally, ψ is chosen to be well localized not only in direct space but also in Fourier space (the scale a can thus be seen as the inverse of a local frequency). Throughout this study, we will use the set of compactly supported analysing wavelets $\psi^{(n)}_{(m)}$ defined in Roux (1996) and Arneodo *et al.* (1997). The $\psi^{(1)}_{(m)}$ are smooth versions of $\psi^{(1)}_{(0)}$ obtained after m successive convolutions with the box function χ. $\psi^{(n)}_{(m)}$ are higher-order analysing wavelets with n vanishing moments. The WT associates to a function in $\mathbb{R}$, its transform defined on $\mathbb{R}\times\mathbb{R}^+$ and is thus very redundant. Following the strategy proposed in Arneodo *et al.* (1997, 1998*c*), we restrict our analysis

to the *modulus maxima* of the WT (WTMM) so that the amount of data to process is more tractable (see figure 1). A straightforward generalization of equation (1.2) in terms of the WTMM PDF at scale a, $P_a(T)$, then reads

$$P_a(T) = \int G_{aa'}(u) P_{a'}(\mathrm{e}^{-u}T)\mathrm{e}^{-u}\,\mathrm{d}u, \quad \text{for } a' > a. \tag{2.2}$$

From (2.2) one can show that, for any decreasing sequence of scales $(a_1, \ldots, a_n)$, the kernel G satisfies the composition law

$$G_{a_n a_1} = G_{a_n a_{n-1}} \otimes \cdots \otimes G_{a_2 a_1}, \tag{2.3}$$

where $\otimes$ denotes the convolution product. According to Castaing and co-workers (Castaing *et al.* 1990; Castaing & Dubrulle 1995), the cascade is *self-similar* if there exists a decreasing sequence of scales $\{a_n\}$ such that $G_{a_n a_{n-1}} = G$ is independent of n. The cascade is said to be *continuously self-similar* if there exists a positive decreasing function $s(a)$ such that $G_{aa'}$ depends on a and a' only through $s(a, a') = s(a) - s(a')$: $G_{aa'}(u) = G(u, s(a, a'))$. $s(a, a')$ actually accounts for the number of elementary cascade steps from scale a' to scale a ($s(a)$ can be seen as the number of cascade steps from the integral scale L down to the considered scale a). In the Fourier space, the convolution property (equation (2.3)) turns into a multiplicative property for $\hat{G}$, the Fourier transform of G:

$$\hat{G}_{aa'}(p) = \hat{G}(p)^{s(a,a')}, \quad \text{for } a' > a. \tag{2.4}$$

From this equation, one deduces that $\hat{G}$ has to be the characteristic function of an infinitely divisible PDF. Such a cascade is referred to as a log-infinitely divisible cascade (Novikov 1990, 1995; Dubrulle 1994; She & Waymire 1995; Castaing & Dubrulle 1995). According to Novikov's definition (Novikov 1990, 1995), the cascade is *scale-similar* (or *scale-invariant*) if

$$s(a, a') = \ln(a'/a), \tag{2.5}$$

i.e. $s(a) = \ln(L/a)$. Let us note that in their original work Castaing *et al.* (1990) developed a formalism, based on an extremum principle, which is consistent with the KO62 general ideas of lognormality (Kolmogorov 1962; Obukhov 1962), but which predicts an anomalous power-law behaviour of the depth of the cascade $s(a) \sim (L/a)^{\beta}$. From the computation of the scaling behaviour of the variance of the kernel $G_{aa'}$, they have checked whether the above-mentioned power-law behaviour could provide a reasonable explanation for the deviation from scaling observed experimentally on the velocity fluctuation statistics (Castaing *et al.* 1990, 1993; Gagne *et al.* 1994; Naert *et al.* 1994; Chabaud *et al.* 1994; Chillà *et al.* 1996).

Our numerical estimation of G (Arneodo *et al.* 1997, 1998*c*) is based on the computation of the characteristic function $M(p, a)$ of the WTMM logarithms at scale a:

$$M(p, a) = \int \mathrm{e}^{\mathrm{i}p \ln |T|} P_a(T)\,\mathrm{d}T. \tag{2.6}$$

From equation (2.2), it is easy to show that $\hat{G}$ satisfies

$$M(p, a) = \hat{G}_{aa'}(p) M(p, a'). \tag{2.7}$$

After the WT calculation and the WTMM detection, the real and imaginary parts of $M(p,a)$ are computed separately as $\langle\cos(p\ln|T|)\rangle$ and $\langle\sin(p\ln|T|)\rangle$, respectively. The use of the WTMM skeleton instead of the continuous WT prevents $M(p,a')$ from getting too small compared with numerical noise over a reasonable range of values of p, so that $\hat{G}_{aa'}(p)$ can be computed from the ratio

$$\hat{G}_{aa'}(p) = \frac{M(p,a)}{M(p,a')}. \tag{2.8}$$

We refer the reader to Roux (1996) and Arneodo *et al.* (1997) for test applications of this method to synthetic turbulent signals.

(*b*) *Experimental determination of the kernel G*

The turbulence data were recorded by Gagne and co-workers in the S1 wind tunnel of ONERA at Modane. The Taylor-scale-based Reynolds number is about $R_\lambda \simeq 2000$ and the Kolmogorov $k^{-5/3}$ law for the energy spectrum approximately holds on an 'inertial range' (in § 5 we propose an objective definition of inertial range on the basis of which the inertial range is significantly less than four decades; we will implicitly use this definition in the remainder of this paper) of about four decades (from the integral scale $L \simeq 7$ m down to the dissipative scale $\eta \simeq 0.27$ mm). The overall statistical sample is about 25×10^7 points long, with a resolution of roughly 3η, corresponding to about 25 000 integral scales. Temporal data are identified to spatial fluctuations of the longitudinal velocity via the Taylor hypothesis (Frisch 1995; Tabeling & Cardoso 1995). Figure 1 illustrates the WT and its skeleton of a sample of the (longitudinal) velocity signal of length of about two integral scales. The analysing wavelet $\psi^{(1)}_{(3)}$ is a first-order compactly supported wavelet. We have checked that all the results reported below are consistent when changing both the regularity and the order of ψ. With the specific goal of investigating the dependence of the statistics on the Reynolds number, we will also report results of similar analysis of wind-tunnel ($R_\lambda \simeq 3050$), jet ($R_\lambda \simeq 800$ and 600) and grid ($R_\lambda \simeq 280$) turbulences, but for statistical samples of smaller sizes.

(i) *Uncovering a continuously self-similar cascade (Arneodo et al. 1998c)*

In order to test the validity of equation (2.4), we first focus on the scale dependence of $\hat{G}_{aa'}$ as calculated with equation (2.8). Figure 2*a* shows the logarithm of the modulus $\ln|\hat{G}_{aa'}|$ and figure 2*b* shows the phase $\phi_{aa'}$ of $\hat{G}_{aa'}$ for various pairs of scales $a < a'$ in the inertial range. In figure 2*c*, *d*, we succeed in collapsing all these different curves onto a single kernel $\hat{G} = \hat{G}^{1/s(a,a')}_{aa'}$, in very good agreement with equation (2.4) and the continuously self-similar cascade picture. In the inserts of figure 2*a*, *b*, we compare our estimation of $\hat{G}_{aa'}$ for the turbulent signal and for a lognormal numerical process of the same length (Arneodo *et al.* 1998*b*). On the numerical lognormal cascade, deviations from the expected parabolic behaviour of $\ln|\hat{G}_{aa'}|$, as well as from the linear behaviour of $\phi_{aa'}$ (see equation (2.12)), become perceptible for $|p| > 5$. Very similar features are observed for the turbulence data, showing that the slight dispersion at large values of p on the curves in figure 2*c*, *d* can be attributed to a lack of statistics. Thus, from now on, we will restrict our analysis of $\hat{G}(p)$ to $p \in [-4, 4]$.

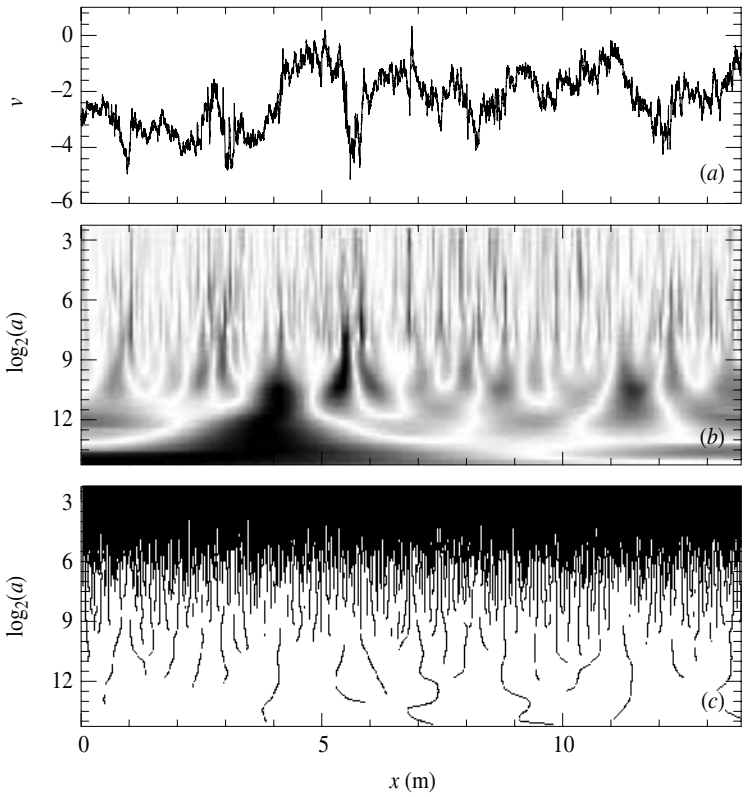

Figure 1. Continuous WT of fully developed turbulence data from the wind-tunnel experiment ($R_\lambda \simeq 2000$). (*a*) The turbulent velocity signal over about two integral scales. (*b*) WT of the turbulent signal; the amplitude is coded, independently at each scale a, using 32 grey levels from white ($|T_\psi[v](x,a)| = 0$) to black ($\max_x |T_\psi[v](x,a)|$). (*c*) WT skeleton defined by the set of all the WTMM lines. In (*b*) and (*c*), the small scales are at the top. The analysing wavelet is $\psi^{(1)}_{(3)}$.

In order to test scale-similarity or more generally the pertinence of equation (2.4), we plot in figure $3a, c$,

$$m(a,a') = \partial \frac{\mathrm{Im}(\hat{G}_{aa'})}{\partial p}\bigg|_{p=0} \quad \text{and} \quad \sigma^2(a,a') = -\frac{\partial^2(\ln|\hat{G}_{aa'}|)}{\partial p^2}\bigg|_{p=0},$$

respectively, as functions of $s(a,a') = \ln(a'/a)$ for different couples of scales (a,a') in the inertial range. It is striking for the jet data ($R_\lambda \simeq 800$), but also noticeable for the wind-tunnel data ($R_\lambda \simeq 3050$), that the curves obtained when fixing the largest scale a' and varying the smallest scale a, have a clear bending and do not merge on the same straight line as expected for scale-similar cascade processes. In figure $3b, d$, the same data are plotted versus $s(a,a') = (a^{-\beta} - a'^{-\beta})/\beta$ with $\beta = 0.08$ for the wind-tunnel flow and $\beta = 0.19$ for the jet flow. In this case, the data for the mean $m(a,a')$ and the variance $\sigma^2(a,a')$ fall, respectively, on a unique line. Those velocity fields are therefore not scale-similar but rather are characterized by some anomalous behaviour of the number of cascade steps between scale a' and scale a:

$$s(a,a') = (a^{-\beta} - a'^{-\beta})/\beta, \tag{2.9}$$

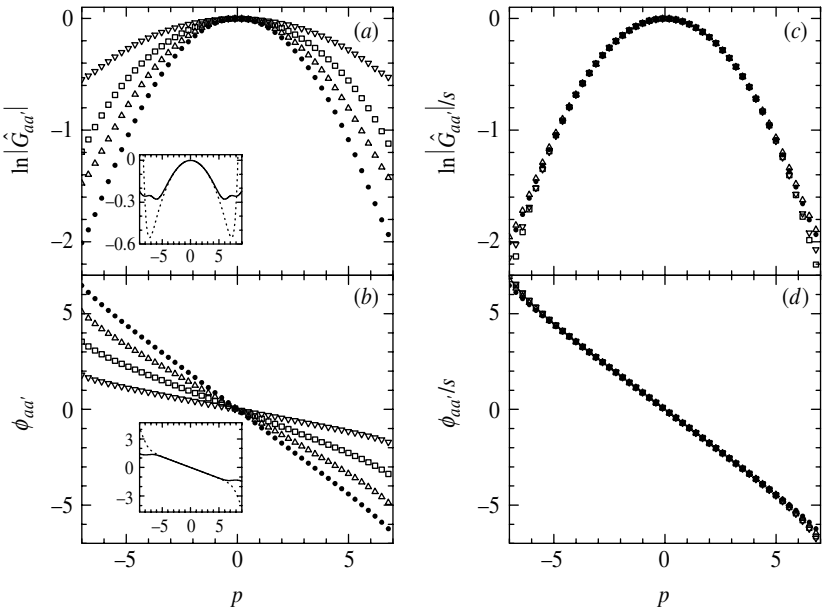

Figure 2. Estimation of $\hat{G}_{aa'}(p)$ for the Modane turbulent velocity signal ($R_\lambda \simeq 2000$) using equation (2.8). The analysing wavelet is $\psi^{(1)}_{(3)}$. (*a*) $\ln|\hat{G}_{aa'}(p)|$ versus p. (*b*) $\phi_{aa'}(p)$ versus p for: $a = 271\eta$, $a' = 4340\eta$ (•); $a = 385\eta$, $a' = 3080\eta$ (△); $a = 540\eta$, $a' = 2170\eta$ (□); $a = 770\eta$, $a' = 1540\eta$ (▽). Inserts: the experimental $\hat{G}_{aa'}(p)$ for $a = 770\eta$ and $a' = 1540\eta$ (dotted line) compared with the computation of $\hat{G}_{aa'}(p)$ for a lognormal numerical process of parameters $m = 0.39$ and $\sigma^2 = 0.036$ with $a = 2^8$ and $a' = 2^9$ (solid line). (*c*) and (*d*) The same curves after being rescaled by a factor of $1/s(a, a')$ with $s = 1$ (•), $s = 0.754$ (△), $s = 0.508$ (□), $s = 0.254$ (▽).

where the exponent β somehow quantifies the departure from scale-similarity (scale-invariance being restored for $\beta \to 0$).† Let us point out that equation (2.9) differs from the pure power law prompted by Castaing and co-workers (Castaing *et al.* 1990, 1993; Gagne *et al.* 1994; Naert *et al.* 1994; Chabaud *et al.* 1994; Chillà *et al.* 1996), since when fixing the reference scale a', the number of cascade steps required to reach the scale a is not exactly $a^{-\beta}/\beta$, but some corrective term $-a'^{-\beta}/\beta$, which has to be taken into account.

(ii) *Discriminating between lognormal and log-Poisson cascades (Arneodo et al. 1998c)*

The relevance of equation (2.4) being established, let us turn to the precise analysis of the nature of G. Using the Taylor-series expansion of $\ln \hat{G}(p)$,

$$\hat{G}(p) = \exp\left(\sum_{k=1}^{\infty} c_k \frac{(\mathrm{i}p)^k}{k!}\right), \tag{2.10}$$

† Note that in order to collapse all the curves onto a single curve in figure 2*c*, *d*, equation (2.9) was used with $\beta = 0.095$.

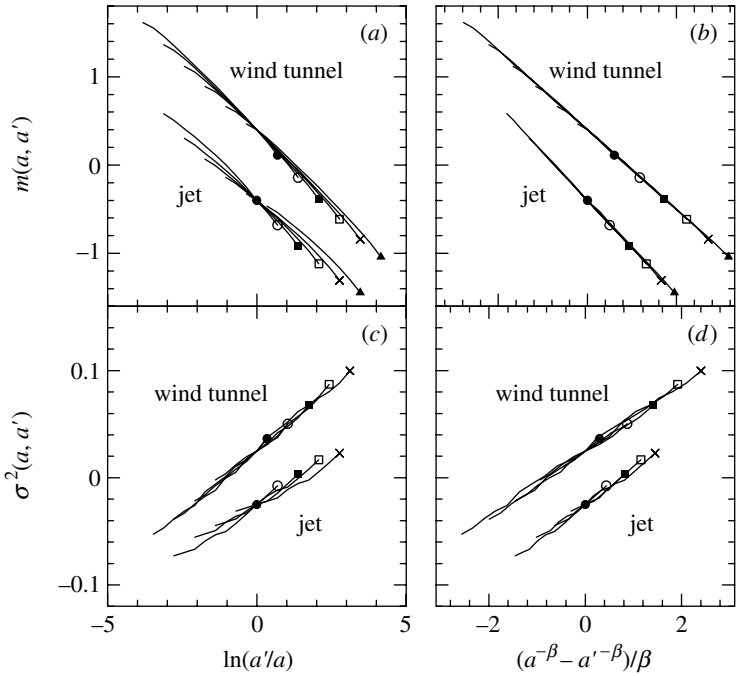

Figure 3. $m(a, a')$ and $\sigma^2(a, a')$ as computed for the jet ($R_\lambda \simeq 800$) and wind-tunnel ($R_\lambda \simeq 3050$) velocity signals for $a' = 2^6$ (•), 2^7 (○), 2^8 (■), 2^9 (□), 2^{10} (×). (*a*) $m(a, a')$ versus $\ln(a'/a)$; (*b*) $m(a, a')$ versus $(a^{-\beta} - a'^{-\beta})/\beta$; (*c*) $\sigma^2(a, a')$ versus $\ln(a'/a)$; (*d*) $\sigma^2(a, a')$ versus $(a^{-\beta} - a'^{-\beta})/\beta$. In (*b*) and (*d*), $\beta = 0.19$ (jet) and $\beta = 0.08$ (wind tunnel).

equation (2.4) can be rewritten as

$$\hat{G}_{aa'}(p) = \exp\left(\sum_{k=1}^{\infty} s(a, a') c_k \frac{(\mathrm{i}p)^k}{k!}\right), \tag{2.11}$$

where the (real-valued) coefficients c_k are the cumulants of G.

(i) Lognormal cascade process (Kolmogorov 1962; Obukhov 1962): a lognormal cascade is characterized by a Gaussian kernel (Roux 1996; Arneodo *et al.* 1997)

$$\hat{G}_{aa'}(p) = \exp[s(a, a')(-\mathrm{i}mp - \tfrac{1}{2}\sigma^2 p^2)], \tag{2.12}$$

which corresponds to the following set of cumulants:

$$c_1 = -m, \quad c_2 = \sigma^2 \quad \text{and} \quad c_k = 0 \quad \text{for } k \geqslant 3. \tag{2.13}$$

(ii) Log-Poisson cascade process (Dubrulle 1994; Castaing & Dubrulle 1995; She & Waymire 1995): a log-Poisson cascade is characterized by the following kernel shape (Roux 1996; Arneodo *et al.* 1997):

$$\hat{G}_{aa'}(p) = \exp[s(a, a')(\lambda(\cos(p \ln \delta) - 1) + \mathrm{i}(p\gamma + \lambda \sin(p \ln \delta)))], \tag{2.14}$$

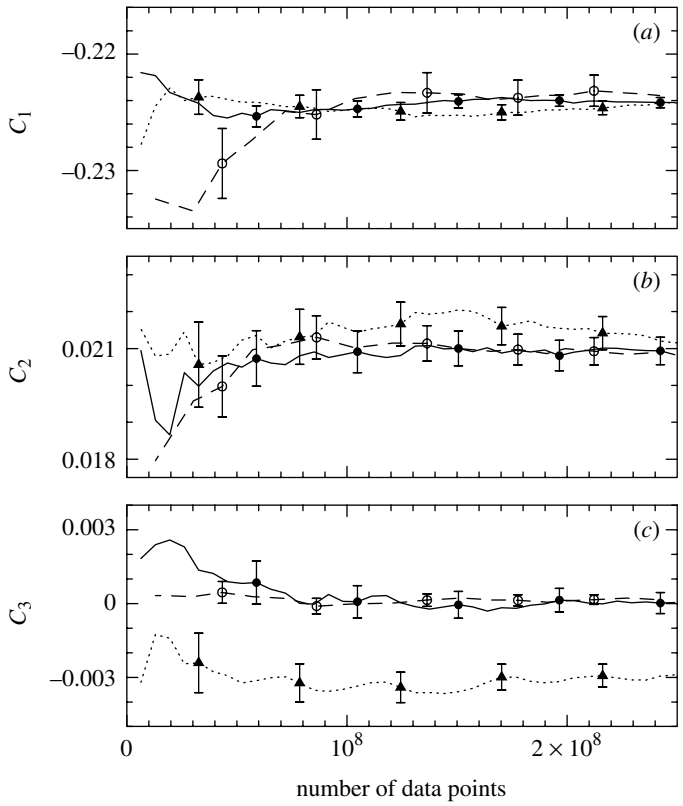

Figure 4. The first three cumulants of $G_{aa'}$ versus the sample length. Turbulent velocity signal for $a = 770\eta$ and $a' = 1540\eta$ (∘ and dashed line), lognormal numerical process of parameters $m = 0.39$ and $\sigma^2 = 0.036$ (• and solid line) and log-Poisson numerical process of parameters $\lambda = 2$, $\delta = 0.89$ and $\gamma = -0.082$ (▲ and dotted line) for the two corresponding scales $a = 2^8$ and $a' = 2^9$. Error bars are estimates of the RMS deviations of the cumulants from their asymptotical values.

where λ, δ and γ are parameters. This log-Poisson kernel corresponds to the following set of cumulants:

$$c_1 = \gamma + \lambda \ln \delta \quad \text{and} \quad c_k = \lambda \frac{(\ln \delta)^k}{k!} \quad \text{for } k \geqslant 2. \tag{2.15}$$

Note that the log-Poisson process reduces to a lognormal cascade for $|p \ln \delta| \ll 1$, i.e. in the limit $\delta \to 1$, where the atomic nature of the quantized log-Poisson process vanishes.

For a given pair of inertial scales $a < a'$, we proceed to polynomial fits of $\ln |\hat{G}_{aa'}(p)|$ and $\phi_{aa'}(p)$, prior to the use of equation (2.11) to estimate the first three cumulants $C_k = s(a, a')c_k$ as a function of the statistical sample length for the wind-tunnel turbulence data at $R_\lambda \simeq 2000$ and for both a lognormal and a log-Poisson synthetic numerical process. Figure 4 shows that statistical convergence is achieved up to the third-order coefficient. However, our sample total length does not allow us to reach statistical convergence for higher-order cumulants. Note that the third cumu-

lant computed for a synthetic lognormal process with parameters m and σ^2 chosen equal to the asymptotic values of C_1 and C_2 (figure 4*a*, *b*), namely $m = 0.39$ and $\sigma^2 = 0.036$, cannot be distinguished from the experimental C_3 (figure 4*c*). In the log-Poisson model, by setting $\lambda = 2$ (according to She & Leveque (1994), λ is the codimension of the most intermittent structures that are assumed to be filaments), we are able to find values of δ and γ close to those proposed in She & Leveque (1994) ($\delta = (\frac{2}{3})^{1/3}$ and $\gamma = -\frac{1}{9}$) that perfectly fit the first two cumulants. However, as seen in figure 4*c*, this set of parameters yields a third-order cumulant that is more than one order of magnitude larger than the experimental cumulant. Actually, when taking λ as a free parameter, good log-Poisson approximations of the first three cumulants are obtained for unrealistic values of λ of order 100 and for values of δ very close to 1, i.e. when the log-Poisson process reduces to the lognormal model. From these results, we conclude that, for the analysed wind-tunnel velocity signal ($R_\lambda \simeq 2000$), G is a Gaussian kernel since $C_3 = 0$ implies $C_k = 0$ for $k > 2$. Therefore, the large size of our statistical sample allows us to exclude log-Poisson statistics with the parameters proposed in She & Leveque (1994).

3. Experimental evidence for a non-scale-invariant lognormal cascading process in high-Reynolds-number turbulent flows

(*a*) *Space-scale correlation functions from wavelet analysis*

Correlations in multifractals have already been experienced in the literature (Cates & Deutsch 1987; Siebesma 1988; Neil & Meneveau 1993). However, all these studies rely upon the computation of the scaling behaviour of some partition functions involving different points; they thus mainly concentrate on spatial correlations of the local singularity exponents. The approach developed in Arneodo *et al.* (1998*a*) is different since it does not focus on (nor suppose) any scaling property but rather consists in studying the correlations of the *logarithms* of the amplitude of a space-scale decomposition of the signal. For that purpose, the wavelet transform is a natural tool to perform space-scale analysis. More specifically, if $\chi(x)$ is a bump function such that $||\chi||_1 = 1$, then by taking

$$\Sigma^2(x,a) = a^{-2} \int \chi((x-y)/a)|T_\psi[v](y,a)|^2 \,\mathrm{d}y, \tag{3.1}$$

one has

$$||v||_2^2 = \iint \Sigma^2(x,a) \,\mathrm{d}x \,\mathrm{d}a, \tag{3.2}$$

and thus $\Sigma^2(x,a)$ can be interpreted as the local space-scale energy density of the considered velocity signal v (Morel-Bailly *et al.* 1991). Since $\Sigma^2(x,a)$ is a positive quantity, we can define the *magnitude* of the field v at point x and scale a as

$$\omega(x,a) = \tfrac{1}{2} \ln \Sigma^2(x,a). \tag{3.3}$$

Our aim in this section is to show that a cascade process can be studied through the correlations of its space-scale magnitudes (Arneodo *et al.* 1998*a*):

$$C(x_1,x_2,a_1,a_2) = \overline{\tilde{\omega}(x_1,a_1)\tilde{\omega}(x_2,a_2)}, \tag{3.4}$$

where the overline stands for ensemble average and $\tilde{\omega}$ for the centred process $\omega - \overline{\omega}$.

(*b*) *Analysis of random cascades using space-scale correlation functions (Arneodo et al. 1998a, b)*

Cascade processes can be defined in various ways. Periodic wavelet orthogonal bases (Meyer 1990; Daubechies 1992) provide a general framework in which they can be constructed easily (Benzi *et al.* 1993*a*; Roux 1996; Arneodo *et al.* 1997, 1998*b*, *c*). Let us consider the following wavelet series:

$$f(x) = \sum_{j=0}^{+\infty} \sum_{k=0}^{2^j-1} c_{j,k}\psi_{j,k}(x), \tag{3.5}$$

where the set $\{\psi_{j,k}(x) = 2^{j/2}\psi(2^j x - k)\}$ is an orthonormal basis of $L^2([0, L])$ and the coefficients $c_{j,k}$ correspond to the WT of f at scale $a = L2^{-j}$ (L is the 'integral' scale that corresponds to the size of the support of $\psi(x)$) and position $x = ka$. The above sampling of the space-scale plane defines a dyadic tree (Meyer 1990; Daubechies 1992). If one indexes by a dyadic sequence $\{\epsilon_1, \ldots, \epsilon_j\}$ ($\epsilon_k = 0$ or 1), with each of the 2^j nodes at depth j of this tree, the cascade is defined by the multiplicative rule:

$$c_{j,k} = c_{\epsilon_1 \ldots \epsilon_j} = c_0 \prod_{i=1}^{j} W_{\epsilon_i}.$$

The law chosen for the weights W (accounting for their possible correlations) determines the nature of the cascade and the multifractal (regularity) properties of f (Benzi *et al.* 1993*a*; Arneodo *et al.* 1998*b*). From the above multiplicative structure, if one assumes that there is no correlation between the weights at a given cascade step, then it is easy to show that for $a_p = L2^{-j_p}$ and $x_p = k_p a_p$ ($p = 1$ or 2), the correlation coefficient is simply the variance $V(j)$ of $\ln c_{j,k} = \sum \ln W_{\epsilon_i}$, where (j, k) is the deepest common ancestor to the nodes (j_1, k_1) and (j_2, k_2) on the dyadic tree (Arneodo *et al.* 1998*a*, *b*). This 'ultrametric' structure of the correlation function shows that such a process is not stationary (nor ergodic). However, we will generally consider uncorrelated consecutive realizations of length L of the same cascade process, so that, in good approximation, C depends only on the space lag $\Delta x = x_2 - x_1$ and one can replace ensemble average by space average. In that case, $C(\Delta k, j_1, j_2) = \langle C(k_1, k_1 + \Delta k, j_1, j_2)\rangle$ can be expressed as

$$C(\Delta k, j_1, j_2) = 2^{-(j-n)} \sum_{p=1}^{j-n} 2^{j-n-p} V(j - n - p), \tag{3.6}$$

where $j = \sup(j_1, j_2)$ and $n = \log_2 \Delta k$. Let us illustrate these features on some simple cases (Arneodo *et al.* 1998*a*, *b*).

(i) *Scale-invariant random cascades*

First let us choose, as in classical cascades, i.i.d. random variables $\ln W_{\epsilon_i}$ of variance λ^2 (e.g. lognormal). Then $V(j) = \lambda^2 j$ and it can be established that, for $\sup(a_1, a_2) \leqslant \Delta x < L$,

$$C(\Delta x, a_1, a_2) = \lambda^2 \left(\log_2 \left(\frac{L}{\Delta x} \right) - 2 + 2\frac{\Delta x}{L} \right). \tag{3.7}$$

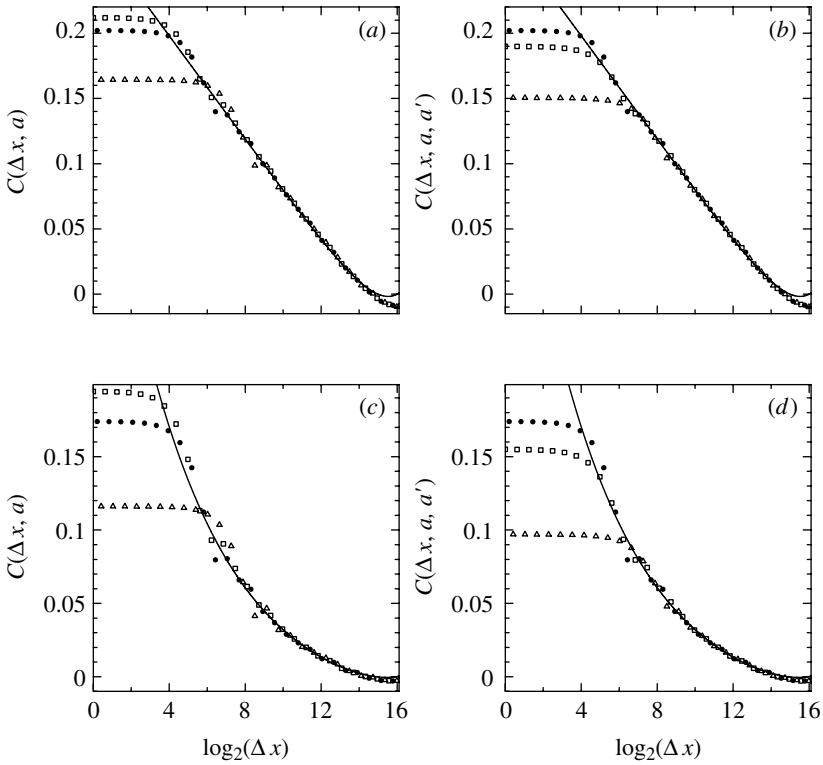

Figure 5. Numerical computation of magnitude correlation functions for lognormal cascade processes built on an orthonormal wavelet basis. Scale-invariant cascade: (*a*) 'one-scale' correlation functions $C(\Delta x, a, a)$ for $a = 4$ (□), 16 (•) and 64 (△); (*b*) 'two-scale' correlation functions $C(\Delta x, a, a')$ for $a = a' = 16$ (•), $a = 4$, $a' = 16$ (□) and $a = 16$, $a' = 64$ (△). The solid lines represent fits of the data with the lognormal prediction (equation (3.7)) using the parameters $\lambda^2 = 0.03$ and $\log_2 L = 16$. Non-scale-invariant cascade: (*c*) 'one-scale' correlation functions; (*d*) 'two-scale' correlation functions. Symbols have the same meaning as in (*a*) and (*b*). The solid lines correspond to equation (3.8) with $\beta = 0.3$, $\lambda^2 = 0.2$ and $\log_2 L = 16$.

Thus, the correlation function decreases very slowly, independently of a_1 and a_2, as a logarithm function of Δx. This behaviour is illustrated in figure 5*a*, *b*, where a lognormal cascade has been constructed using Daubechies compactly supported wavelet basis (D-5) (Arneodo *et al.* 1998*b*). The correlation functions of the magnitudes of $f(x)$ have been computed as described above (equation (3.4)) using a simple box function for $\chi(x)$. Let us note that all the results reported in this section concern the increments of the considered signal and that we have checked that they are actually independent of the specific choice of the analysing wavelet ψ. In figure 5*a* are plotted the 'one-scale' ($a_1 = a_2 = a$) correlation functions for three different scales $a = 4$, 16 and 64. One can see that, for $\Delta x > a$, all the curves collapse to a single curve, which is in perfect agreement with expression (3.7): in semi-log-coordinates, the correlation functions decrease almost linearly (with slope λ^2) up to the integral scale L, that is of order 2^{16} points. In figure 5*b* are displayed these correlation functions when the two scales a_1 and a_2 are different. One can check that, as expected, they still do not depend on the scales provided $\Delta x \geqslant \sup(a_1, a_2)$; moreover, they are again very well

fitted by the above theoretical curve (except at very large Δx where finite size effects show up). The linear behaviour of $C(\Delta x, a_1, a_2)$ versus $\ln(\Delta x)$ is characteristic for 'classical' scale-invariant cascades for which the random weights are uncorrelated.

(ii) *Non-scale-invariant random cascades*

One can also consider non-scale-invariant cascades where the weights are not identically distributed and have an explicit scale dependence (Arneodo *et al.* 1998*a*). For example, we can consider a lognormal model whose coefficients $\ln c_{j,k}$ have a variance that depends on j as $V(j) = \lambda^2(2^{j\beta} - 1)/(\beta \ln 2)$. This model is inspired by the ideas of Castaing and co-workers (Castaing *et al.* 1990, 1993; Gagne *et al.* 1994; Naert *et al.* 1994; Chabaud *et al.* 1994; Castaing & Dubrulle 1995; Chillà *et al.* 1996) and the experimental results reported in § 2. Note that it reduces to a scale-invariant model in the limit $\beta \to 0$. For finite β and $\sup(a_1, a_2) \leqslant \Delta x < L$, the correlation function becomes

$$C(\Delta x, a_1, a_2) = \frac{\lambda^2}{\beta \ln 2}\left(\frac{(L/\Delta x)^\beta - (\Delta x/L)}{2^{\beta+1} - 1} - 1 + \frac{\Delta x}{L}\right). \tag{3.8}$$

As for the first example, we have tested our formalism on this model constructed using the same Daubechies wavelet basis and considering, for the sake of simplicity, i.i.d. lognormal weights W_{ϵ_i}. Figure 5*c*, *d* is the analogue of figure 5*a*, *b*. One can see that, when scale-invariance is broken, our estimates of the magnitude correlation functions are in perfect agreement with equation (3.8), which predicts a power-law decrease of the correlation functions versus Δx.

(iii) *Distinguishing 'multiplicative' from 'additive' processes (Arneodo et al. 1998a)*

The two previous examples illustrate the fact that magnitudes in random cascades are correlated over very long distances. Moreover, the slow decay of the correlation functions is independent of scales for large enough space lags ($\Delta x > a$). This is reminiscent of the multiplicative structure along a space-scale tree. These features are not observed in 'additive' models like fractional Brownian motions whose long-range correlations originate from the sign of their variations rather than from the amplitudes. In figure 6 are plotted the correlation functions of an 'uncorrelated' lognormal model constructed using the same parameters as in the first example but without any multiplicative structure (the coefficients $c_{j,k}$ have, at each scale j, the same lognormal law as before but are independent) and for a fractional Brownian motion with $H = \frac{1}{3}$. Let us note that from the point of view of both the multifractal formalism and the increment PDF scale properties, the 'uncorrelated' and 'multiplicative' lognormal models are indistinguishable since their one-point statistics at a given scale are identical. As far as the magnitude space-scale correlations are concerned, the difference between the cascade and the other models is striking: for $\Delta x > a$, the magnitudes of the fractional Brownian motion and of the lognormal 'white-noise' model are found to be uncorrelated.

(*c*) *Analysis of velocity data using space-scale correlation functions (Arneodo et al. 1998a)*

In this subsection, we report preliminary application of space-scale correlation functions to Modane wind-tunnel velocity data at $R_\lambda \simeq 2000$, which correspond to

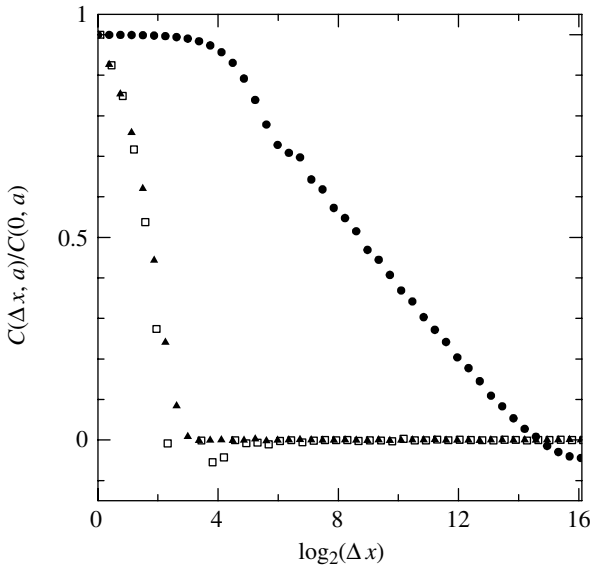

Figure 6. 'One-scale' ($a = 4$) magnitude correlation functions: lognormal cascade process (●); lognormal 'white noise' (□); $H = \frac{1}{3}$ fractional Brownian motion (▲). Magnitudes are correlated over very long distances for the cascade process while they are uncorrelated when $\Delta x > a$ for the two other processes.

the highest statistics accessible to numerical analysis. In figure $7a, b$ are plotted (to be compared with figure 5) the 'one-scale' and 'two-scale' correlation functions. Both figures clearly show that space-scale magnitudes are strongly correlated. Very much like previous toy cascades, it seems that for $\Delta x > a$, all the experimental points $C(\Delta x, a_1, a_2)$ fall onto a single curve. We find that this curve is nicely fitted by equation (3.8) with $\beta = 0.3$, $\lambda^2 = 0.27$ and $L \simeq 2^{14}$ points. This latter length-scale corresponds to the integral scale of the experiment that can be estimated from the power spectrum. It thus seems that the space-scale correlations in the magnitude of the velocity field are in very good agreement with a cascade model that is not scale-invariant. This corroborates the results of § 2 from 'one-point' statistical studies. However, we have observed several additional features that do not appear in wavelet cascades. (i) For $\Delta x > L$, the correlation coefficient is not in the noise level ($C = 0$ as expected for uncorrelated events) but remains negative up to a distance of about three integral scales. This observation can be interpreted as an anticorrelation between successive eddies: very intense eddies are followed by weaker eddies and vice versa. (ii) For $\Delta x \simeq a$, there is a crossover from the value $C(\Delta x = 0, a, a)$ (which is simply the variance of ω at scale a) down to the fitted curve corresponding to the cascade model. This was not the case in previous cascade models (figure 5). This observation suggests that simple self-similar (even non-scale-invariant) cascades are not sufficient to account for the space-scale structure of the velocity field. The interpretation of this feature in terms of correlations between weights at a given cascade step or in terms of a more complex geometry of the tree underlying the energy cascade is under progress. The possible importance of spatially fluctuating viscous smoothing effects (Frisch & Vergassola 1991) is also under consideration.

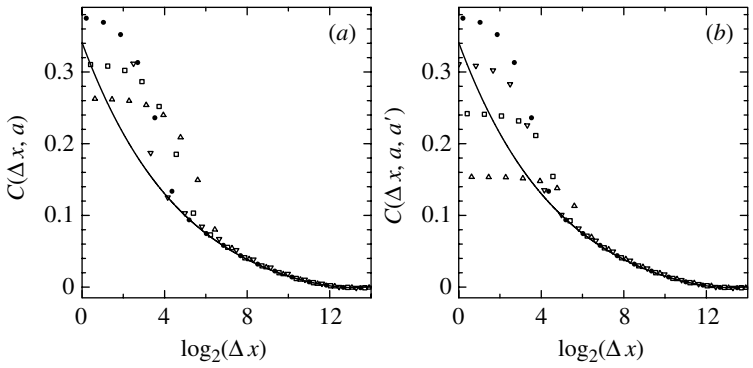

Figure 7. Magnitude correlation functions of Modane fully developed turbulence data ($R_\lambda \simeq 2000$): (*a*) 'one-scale' correlation functions at scales $a = 24\eta$ ($\triangledown$), 48η ($\bullet$), 96η ($\square$) and 192η ($\triangle$); (*b*) 'two-scale' correlations functions at scales $a = 24\eta$, $a' = 48\eta$ ($\triangledown$), $a = 48\eta$, $a' = 48\eta$ ($\bullet$), $a = 48\eta$, $a' = 96\eta$ ($\square$) and $a = 48\eta$, $a' = 192\eta$ ($\triangle$). The solid lines correspond to a fit using equation (3.8) with $\beta = 0.3$, $\lambda^2 = 0.27$ and $\log_2 L = 13.6$.

4. The multifractal description of intermittency revisited with wavelets

(*a*) *WTMM probability density functions (Arneodo et al. 1998c)*

A first way to check the consistency of our results is to test the convolution formula (2.2) on the WTMM PDFs using a Gaussian kernel. The results of this test application are reported in figure 8 (Arneodo *et al.* 1998*c*). Let us mention that a naive computation of the PDFs of the (continuous) WT coefficients at different scales in the inertial range (Roux 1996), leads to distributions that are nearly centred with a shape that goes from Gaussian at large scales to stretched exponential-like tails at smaller scales, very much like the evolution observed for the velocity increment PDFs (Gagne 1987; Castaing *et al.* 1990; Kailasnath *et al.* 1992; Frisch 1995; Tabeling *et al.* 1996; Belin *et al.* 1996). But the wavelet theory (Meyer 1990; Daubechies 1992) tells us that there exists some redundancy in the continuous WT representation. Indeed, for a given analysing wavelet, there exists a reproducing kernel (Grossmann & Morlet 1984, 1985; Daubechies *et al.* 1986) from which one can express any WT coefficient at a given point x and scale a as a linear combination of the neighbouring WT coefficients in the space-scale half-plane. As emphasized in Muzy *et al.* (1991, 1993, 1994), Mallat & Hwang (1992) and Bacry *et al.* (1993), a way to break free from this redundancy is to use the WTMM representation. In figure 8*a* are reported the results of the computation of the WTMM PDFs when restricting our analysis to the WT skeleton (figure 1*c*) defined by the WT maxima lines. Since by definition the WTMM are different from zero, the so-obtained PDFs decrease very fast to zero at zero, which will make the estimate of the exponents ζ_q tractable for $q < 0$ in § 4 *b*. When plotting $\ln P_a(\ln(|T|))$ versus $\ln|T|$, one gets in figure 8*b* the remarkable result that for any scale in the inertial range all the data points fall, within a good approximation, on a parabola, which is a strong indication that the WTMM have a lognormal distribution. In figure 8*c* we have succeeded in collapsing all the WTMM PDFs, computed at different scales, onto a single curve when using equation (2.2) with a Gaussian kernel $G(u, s(a, a'))$, where $s(a, a')$ is given by equation (2.9) with

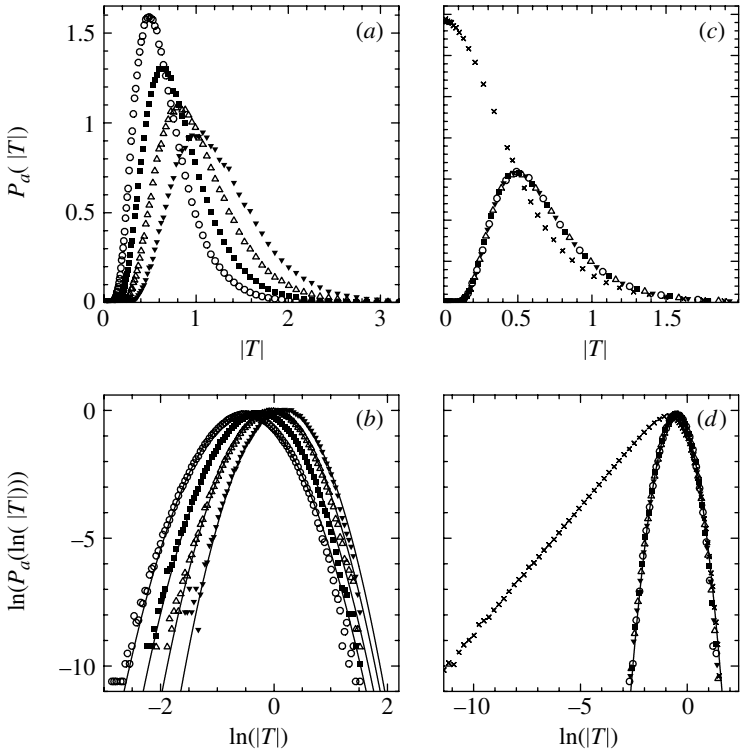

Figure 8. Probability density functions of the WTMM for the Modane turbulent velocity signal ($R_\lambda \simeq 2000$): (*a*) $P_a(|T|)$ versus $|T|$ as computed at different scales $a = 385\eta$ (○), 770η (■), 1540η (△) and 3080η (▼); (*b*) $\ln(P_a(\ln(|T|)))$ versus $\ln|T|$ at the same scales; (*c*) and (*d*) the PDFs after being transformed according to equation (2.2) with a Gaussian kernel $G_{aa'}$ and $s(a,a') = (a^{-\beta} - a'^{-\beta})/\beta$ where $\beta = 0.095$. The (×) in (*c*) and (*d*) represent the velocity increment PDF at scale $a = 308\eta$. The solid lines in (*b*) and (*d*) correspond to the Gaussian approximations of the histograms. The analysing wavelet is $\psi^{(1)}_{(3)}$.

$\beta = 0.095$ in order to account for the scale-invariance breaking mentioned above (§ 2 *b*). This observation corroborates the lognormal cascade picture. Let us point out that, as illustrated in figure 8*c*, *d*, the velocity increment PDFs are likely to satisfy the Castaing and co-workers convolution formula (1.2) with a similar Gaussian kernel, even though their shape evolves across the scales (Roux 1996). The fact that the WTMM PDFs turn out to have a shape which is the fixed point of the underlying kernel has been numerically revealed in previous works (Roux 1996; Arneodo *et al.* 1997) for various synthetic log-infinitely divisible cascade processes. So far, there exists no mathematical demonstration of this remarkable numerical observation.

(*b*) ζ_q *scaling exponents*

A second test of the lognormality of the velocity fluctuations lies in the determination of the ζ_q spectrum. As discussed in previous studies (Muzy *et al.* 1993, 1994), the structure-function approach pioneered by Parisi & Frisch (1985) has several intrinsic insufficiencies which mainly result from the poorness of the underlying analysing wavelet $\psi^{(1)}_{(0)}$. Here we use instead the so-called WTMM method (Muzy *et*

al. 1991, 1993 1994; Bacry *et al.* 1993; Arneodo *et al.* 1995) that has proved to be very efficient in achieving multifractal analysis of very irregular signals. The WTMM method consists of computing the following partition functions:

$$Z(q,a)=\sum_{l\in\mathcal{L}(a)}\left(\sup_{\substack{(x,a')\in l,\\ a'\leqslant a}}|T_\psi[v](x,a')|\right)^q,\quad \forall q\in\mathbb{R}, \tag{4.1}$$

where $\mathcal{L}(a)$ denotes the set of all WTMM lines of the space-scale half-plane that exist at scale a and contain maxima at any scale $a'\leqslant a$. A straightforward analogy with the structure functions $S_q(l)$ (equation (1.1)) yields

$$\mathcal{S}(q,a)=\frac{Z(q,a)}{Z(0,a)}\sim a^{\zeta_q}. \tag{4.2}$$

However, there exist two fundamental differences between $S_q(l)$ and $\mathcal{S}(q,a)$. (i) The summation in equation (4.1) is over the WT skeleton defined by the WTMM. Since by definition the WTMM do not vanish, equation (4.1) allows us to extend the computation of the scaling exponents ζ_q from positive q values only when using the structure functions (as shown in § 4 *a*, the velocity increment PDFs do not vanish at zero), to positive as well as negative q values without any risk of divergences (Muzy *et al.* 1993, 1994). (ii) By considering analysis of wavelets that are regular enough and have some adjustable degree of oscillation, the WTMM method allows us to capture singularities in the considered signal ($0\leqslant h\leqslant 1$) like the structure functions can do, but also in arbitrary high-order derivatives of this signal (Muzy *et al.* 1993, 1994). In that respect, the WTMM method gives access to the entire $D(h)$ singularity spectrum and not only to the strongest singularities as the structure-function method is supposed to do from Legendre transforming ζ_q for $q>0$ only (Muzy *et al.* 1991, 1993 1994; Bacry *et al.* 1993; Arneodo *et al.* 1995).

Since scale-invariance is likely to be broken, one rather expects the more general scale dependence of $\mathcal{S}(q,a)$ (Roux 1996; Arneodo *et al.* 1997, 1999):

$$\mathcal{S}(q,a)=\kappa_q\exp(-\zeta_q s(a)), \tag{4.3}$$

where κ_q is a constant that depends only on q and $s(a)=(a^{-\beta}-1)/\beta$ consistently with the observed anomalous behaviour of $s(a,a')$ given by equation (2.9). Indeed, $\mathcal{S}(q,a)$ can be seen as a generalized mean of $|T|^q$ so that formally, from the definition of the characteristic function $M(q,a)$ (equation (2.6)), one gets

$$\mathcal{S}(q,a)\sim M(-\mathrm{i}q,a). \tag{4.4}$$

From expression (2.8) of the Fourier transform of the kernel G and from equation (4.4), one deduces

$$\frac{\mathcal{S}(q,a)}{\mathcal{S}(q,a')}=\hat{G}_{aa'}(-\mathrm{i}q). \tag{4.5}$$

When further using equation (2.11), this last equation becomes

$$\frac{\mathcal{S}(q,a)}{\mathcal{S}(q,a')}=\exp\left(\sum_{k=1}^{\infty}s(a,a')c_k\frac{q^k}{k!}\right), \tag{4.6}$$

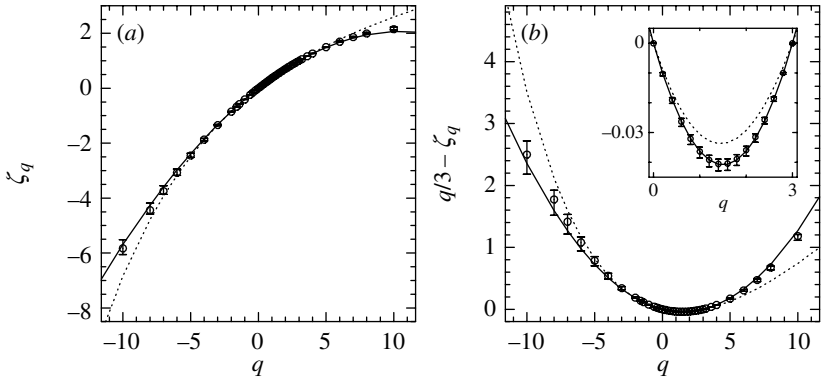

Figure 9. WTMM estimation of the ζ_q spectrum for the Modane turbulent velocity signal ($R_\lambda \simeq 2000$). The analysing wavelet is $\psi^{(1)}_{(3)}$: (*a*) ζ_q versus q; (*b*) deviation of the experimental spectrum from the K41 $\zeta_q = \frac{1}{3}q$ prediction. The experimental ESS measurements ($\circ$) are compared with the theoretical quadratic spectrum of a lognormal process with $m = 0.39$ and $\sigma^2 = 0.036$ (solid line) and to the She & Leveque (1994) log-Poisson prediction with $\lambda = 2$, $\delta = (\frac{2}{3})^{1/3}$ and $\gamma = -\frac{1}{9}$ (dotted line).

which is consistent with equation (4.3) provided that

$$\zeta_q = -\sum_{k=1}^{\infty} \frac{c_k q^k}{k!}. \tag{4.7}$$

We have checked that fitting $\mathcal{S}(q,a)/\mathcal{S}(q,a')$ versus q for the two scales of figure 4 leads to the same estimates of $C_k = s(a,a')c_k$ as above to within less than 1%.

Remark 4.1.

(i) Let us emphasize that for $\psi = \psi^{(1)}_{(0)}$, equation (4.3) is simply the general exponential self-similar behaviour predicted by Dubrulle (1996) (for the structure functions) by simple symmetry considerations.

(ii) As expressed by equation (4.3), the observed breaking of scale-invariance does not invalidate the ESS hypothesis (Benzi *et al.* 1993*b*, 1993*c*, 1995). Actually, equation (4.3) is equivalent to the ESS ansatz.

To estimate the ζ_q spectrum, we thus use the concept of ESS developed by Benzi *et al.* (1993*b*, *c*, 1995) i.e. we set $\zeta_3 = 1$ and plot $\mathcal{S}(q,a) = (\kappa_q/\kappa_3)\mathcal{S}(3,a)^{\zeta_q}$ versus $\mathcal{S}(3,a)$ in log-coordinates (for more details see Arneodo *et al.* (1999)). As shown in figure 9*a*, the experimental spectrum obtained from linear regression procedure remarkably coincides with the quadratic lognormal prediction $\zeta_q = mq - \frac{1}{2}\sigma^2 q^2$ with the same parameters as in § 2 *b* (figure 4), up to $|q| = 10$. We have checked that statistical convergence is achieved for $|q| \leqslant 8$; but even if the convergence becomes questionable for larger values of q, the 'error bars' obtained by varying the range of scales used for the ESS determination of ζ_q show the robustness of the spectrum. Let us point out that the log-Poisson prediction $\zeta_q = -\gamma q + \lambda(1-\delta^q)$, with the She & Leveque (1994) parameter values: $\lambda = 2$, $\delta = (\frac{2}{3})^{1/3}$ and $\gamma = -\frac{1}{9}$, provides a rather good approximation of ζ_q for $q \in [-6, 6]$, in agreement with the structure-function estimations of ζ_q (She & Leveque 1994; She & Waymire 1995; Arneodo

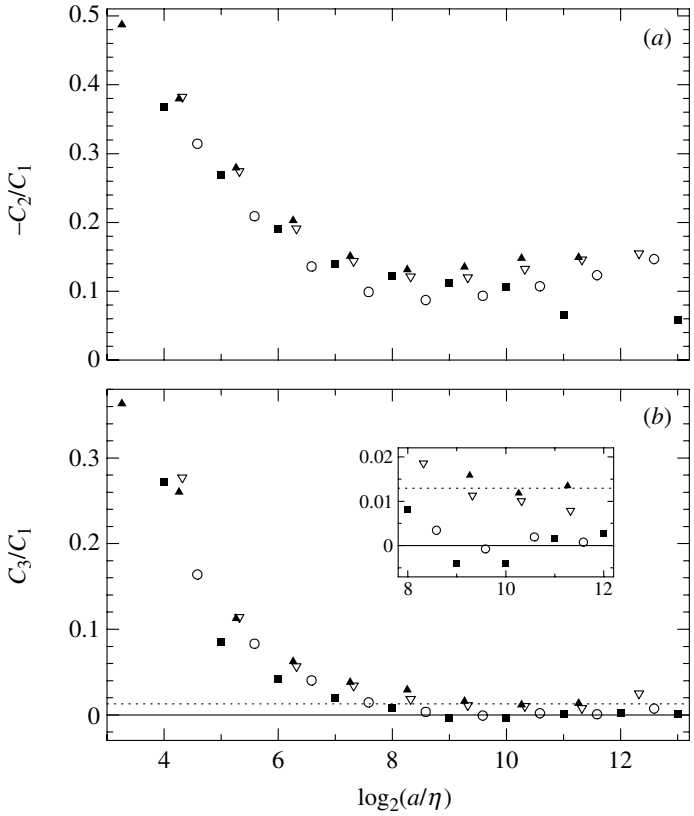

Figure 10. Cumulant ratios $-C_2/C_1$ (a) and C_3/C_1 (b), estimated from $\hat{G}_{aa'}$ with $a' = 2a$, as a function of $\log_2(a/\eta)$ for four turbulent flows of different Reynolds numbers $R_\lambda \simeq 2000$ ($\circ$), 800 ($\triangledown$), 600 ($\blacktriangle$) and 280 ($\blacksquare$). In (b), the solid and dotted lines correspond, respectively, to the lognormal and to the She & Leveque (1994) log-Poisson predictions for C_3/C_1.

et al. 1996; Belin *et al.* 1996) and with our results on the first two cumulants of G (figure 4). However, when plotting the deviation of the ζ_q from the K41 linear $\zeta_q = \frac{1}{3}q$ spectrum (figure 9*b*), one reveals a systematic departure of the log-Poisson prediction from the experimental spectrum, and this even for $q \in [0, 3]$ as shown in the insert of figure 9*b*, whereas the lognormal model still perfectly fits the experimental data. This nicely corroborates our findings on the third-order cumulant of G (figure 4) and shows that very long statistical samples are needed to discriminate between lognormal and log-Poisson statistics in fully developed turbulence data. Note that, according to the quadratic fit reported in figure 9, the ζ_q spectrum should decrease for $q \geqslant 11$, in qualitative agreement with previous discussions (Castaing *et al.* 1990; Belin *et al.* 1996). However, since statistical convergence is not achieved for such high values of q, one has to be careful when extrapolating the ζ_q behaviour. As reported in Belin *et al.* (1996), the number of data points needed to estimate ζ_q increases exponentially fast with q. Reaching an acceptable statistical convergence for $q \simeq 12$ would thus require velocity records about 10 times bigger than those processed in this work.

5. Conclusions and perspectives

To complete our study, we must address the issue of the robustness of our results when one varies the Reynolds number. We have reproduced our WT-based analysis on the turbulent velocity signal at Reynolds number $R_\lambda \simeq 800$ (of about the same length as the previous statistical sample at $R_\lambda \simeq 2000$ and with a resolution of 2.5η) obtained by Gagne *et al.* (1994) in a laboratory jet experiment (Arneodo *et al.* 1998*c*). Because of scale invariance breaking, the notion of inertial range is not well defined. Thus, we may rather call 'inertial range' the range of scales on which equation (2.4) holds with the same kernel G. As illustrated in figure 10, for $R_\lambda \simeq 800$, $C_3/C_1 \simeq 0.01$ is significantly higher than for $R_\lambda \simeq 2000$, whereas $-C_2/C_1$ remains about equal to 0.15. An inertial range can still be defined ($128\eta \leqslant a \leqslant \frac{1}{4}L$), on which $G_{aa'}$ keeps a constant 'inertial' shape, but for $R_\lambda \simeq 800$, this shape becomes compatible with a log-Poisson distribution as proposed in She & Leveque (1994). We have checked that in that case, the She–Leveque model provides a better approximation of the ζ_q spectrum than the lognormal model (Arneodo *et al.* 1998*c*). This result seems to contradict previous studies (Arneodo *et al.* 1996; Belin *et al.* 1996), suggesting that turbulent flows may be characterized by a universal ζ_q spectrum, independent of the Reynolds number, at least for $0 \leqslant q \leqslant 6$. However, as seen in figure 9*a*, for that range of q values, the various models can hardly be distinguished without plotting $q/3 - \zeta_q$. From our WT-based approach, which allows the determination of ζ_q for negative q values, when using very long statistical samples to minimize error bars, we can actually conclude that lognormal statistics no longer provide a perfect description of the turbulent velocity signals at Reynolds numbers $R_\lambda \lesssim 800$. This result, together with previous numerical (Leveque & She 1995, 1997; Benzi *et al.* 1996) and experimental (She & Leveque 1994; Ruiz-Chavarria *et al.* 1995) evidence for the relevance of log-Poisson statistics at low and moderate Reynolds numbers, strongly suggests that there might be some transitory regime ($R_\lambda \lesssim 1000$) towards asymptotic lognormal statistics, which could be accounted for by a quantized log-Poisson cascade or by some other cascade models that predict the correct relative order of magnitude of the higher-order cumulants (mainly c_3 and c_4) of the kernel G (equation (2.10)).

In figure 11 is reported the estimate of the scale-breaking exponent β (equation (2.9)), as a function of the Reynolds number (Arneodo *et al.* 1999); the five points correspond to the results obtained for the two previous experiments and for three additional datasets corresponding to wind-tunnel ($R_\lambda \simeq 3050$), jet ($R_\lambda \simeq 600$) and grid ($R_\lambda \simeq 280$) turbulences. In figure 11*a*, β is plotted versus $1/\ln(R_\lambda)$ in order to check experimentally the validity of some theoretical arguments developed in Castaing *et al.* (1990) and Dubrulle (1996), which predict a logarithmic decay of β when increasing R_λ. Indeed the data are very well fitted by $\beta \sim 1/\ln(R_\lambda) - 1/\ln(R_\lambda^*)$, where $R_\lambda^* \simeq 12\,000$, which suggests that scale-similarity is likely to be attained at finite Reynolds numbers. However, as shown in figure 11*b*, for the range of Reynolds numbers accessible to today experiments the data are equally very well fitted by a power-law decay with an exponent which is close to $\frac{1}{2}$: $\beta \simeq R_\lambda^{-0.556}$. This second possibility brings the clue that scale-similarity might well be valid only in the limit of infinite Reynolds number. Whatever the relevant β behaviour, our findings for the kernel $G_{aa'}$ at $R_\lambda \simeq 2000$ (high statistics in the present work) and 3050 (moderate statistics in Arneodo *et al.* (1997, 1999)), strongly indicate that at very high

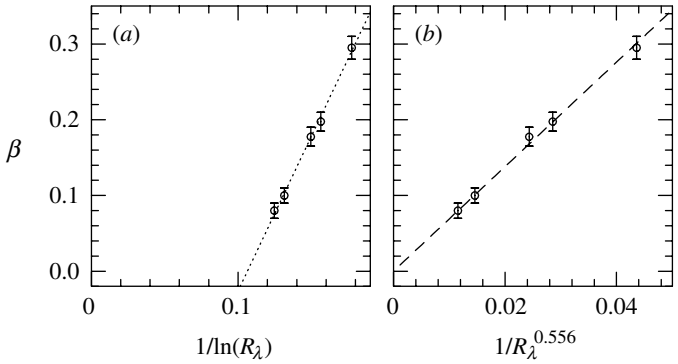

Figure 11. β as a function of the Reynolds number. (a) β versus $1/\ln(R_\lambda)$; the dotted line corresponds to a fit of the data with $\beta = B(1/\ln(R_\lambda) - 1/\ln(R_\lambda^*))$ with $R_\lambda^* = 12\,000$. (b) β versus $R_\lambda^{-0.556}$; the dashed line corresponds to a linear regression fit of the data. Error bars account for variation of β according to the definition of the inertial range.

Reynolds numbers the intermittency phenomenon can be understood in terms of a continuous self-similar multiplicative process that converges towards a scale-similar lognormal cascade.

Remark 5.1. Let us note that in figure 10*b* the estimate of C_3/C_1 for the lowest Reynolds-number velocity signal ($R_\lambda \simeq 280$) we have at our disposal cannot be distinguished from the results obtained for the wind-tunnel experiment at $R_\lambda \simeq 2000$. This observation of lognormal statistics at low Reynolds number contradicts the above conclusions. This might well be the consequence of the presence of some anisotropy at large scales in this grid turbulence where the velocity increment PDFs were found to depart significantly from a symmetric Gaussian shape (Gagne & Malecot, personal communication).

To summarize, this study has revealed the existence of a scale domain that we call 'inertial range', where a high-Reynolds-number turbulent-velocity signal ($R_\lambda \simeq 2000$) displays lognormal statistics. Our results confirm the relevance of the continuously self-similar lognormal cascade picture initiated by Castaing and co-workers (Castaing *et al.* 1990, 1993; Gagne *et al.* 1994; Naert *et al.* 1994; Chabaud *et al.* 1994; Castaing & Dubrulle 1995; Chillà *et al.* 1996). We also emphasize the fact that such an analysis requires very long statistical samples in order to get a good convergence of the cumulants of the kernel G and of the ζ_q spectrum. Our last results about the dependence of the statistics on the Reynolds number suggest that perfect lognormality may be reached only for $R_\lambda \to \infty$. A similar result is obtained concerning the breaking of scale-invariance (Roux 1996; Arneodo *et al.* 1997, 1998*c*, 1999): scale-invariance is likely to be restored only for very large Reynolds numbers. As emphasized by Frisch (1995), scale-invariance together with lognormal statistics for the velocity fluctuations imply that the Mach number of the flow increases indefinitely, which violates a basic assumption needed in deriving the incompressible Navier–Stokes equations. Let us note that this observation does not, however, violate the basic laws of hydrodynamics since it is conceivable that, at extremely high Reynolds numbers, supersonic velocity may appear. A systematic investigation of the evolution of the statistics with both the scale range and the Reynolds number is currently under progress. Further analysis of numerical and experimental data should provide new insights on

the departure of $G_{aa'}$ from its 'inertial' shape outside the inertial range and on the way it converges towards a Gaussian kernel at high Reynolds numbers.

We are very grateful to Y. Gagne and Y. Malecot for the permission to use their experimental turbulent signals. We acknowledge very stimulating discussions with E. Bacry, B. Castaing, S. Ciliberto, Y. Couder, S. Douady, B. Dubrulle, Y. Gagne, F. Graner, J. F. Pinton, P. Tabeling and H. Willaime. This work was supported by 'Direction des Recherches, Etudes et Techniques' under contract DRET no. 95/111.

References

Anselmet, F., Gagne, Y., Hopfinger, E. & Antonia, R. 1984 *J. Fluid. Mech.* **140**, 63.

Arneodo, A., Bacry, E. & Muzy, J. 1995 *Physica* A **213**, 232.

Arneodo, A. (and 24 others) 1996 *Europhys. Lett.* **34**, 411.

Arneodo, A., Muzy, J. & Roux, S. 1997 *J. Physique* II **7**, 363.

Arneodo, A., Bacry, E., Manneville, S. & Muzy, J. 1998*a* *Phys. Rev. Lett.* **80**, 708.

Arneodo, A., Bacry, E. & Muzy, J. 1998*b* *J. Math. Phys.* **39**, 4142.

Arneodo, A., Manneville, S. & Muzy, J. 1998*c* *Eur. Phys. Jl* B **1**, 129.

Arneodo, A., Manneville, S., Muzy, J. & Roux, S. 1999 *Appl. Comput. Harmonic Analysis* **6**, 374.

Bacry, E., Muzy, J. & Arneodo, A. 1993 *J. Statist. Phys.* **70**, 635.

Belin, F., Tabeling, P. & Willaime, H. 1996 *Physica* D **93**, 52.

Benzi, R., Biferale, L., Crisanti, A., Paladin, G., Vergassola, M. & Vulpiani, A. 1993*a* *Physica* D **65**, 352.

Benzi, R., Ciliberto, S., Trippiccione, R., Baudet, C., Massaioli, F. & Succi, S. 1993*b* *Phys. Rev.* E **48**, R29.

Benzi, R., Ciliberto, S., Baudet, C., Ruiz-Chavarria, G. & Trippiccione, R. 1993*c* *Europhys. Lett.* **24**, 275.

Benzi, R., Ciliberto, S., Baudet, C. & Ruiz-Chavarria, G. 1995 *Physica* D **80**, 385.

Benzi, R., Biferale, L. & Trovatore, E. 1996 *Phys. Rev. Lett.* **77**, 3114.

Briscolini, M., Santangelo, P., Succi, S. & Benzi, R. 1994 *Phys. Rev.* E **50**, R1745.

Castaing, B. & Dubrulle, B. 1995 *J. Physique* II **5**, 895.

Castaing, B., Gagne, Y. & Hopfinger, E. 1990 *Physica* D **46**, 177.

Castaing, B., Gagne, Y. & Marchand, M. 1993 *Physica* D **68**, 387.

Cates, M. & Deutsch, J. 1987 *Phys. Rev.* A **35**, 4907.

Chabaud, B., Naert, A., Peinke, J., Chillà, F., Castaing, B. & Hebral, B. 1994 *Phys. Rev. Lett.* **73**, 3227.

Chillà, F., Peinke, J. & Castaing, B. 1996 *J. Physique* II **6**, 455.

Daubechies, I. 1992 *Ten lectures on wavelets.* Philadelphia, PA: SIAM.

Daubechies, I., Grossmann, A. & Meyer, Y. 1986 *J. Math. Phys.* **27**, 1271.

Dubrulle, B. 1994 *Phys. Rev. Lett.* **73**, 959.

Dubrulle, B. 1996 *J. Physique* II **6**, 1825.

Frisch, U. 1995 *Turbulence.* Cambridge University Press.

Frisch, U. & Orzag, S. 1990 *Physics Today*, January, p. 24.

Frisch, U. & Vergassola, M. 1991 *Europhys. Lett.* **14**, 439.

Gagne, Y. 1987 PhD thesis. University of Grenoble.

Gagne, Y., Marchand, M. & Castaing, B. 1994 *J. Physique* II **4**, 1.

Grossmann, A. & Morlet, J. 1984 *SIAM Jl Math. Analyt. Appl.* **15**, 723.

Grossmann, A. & Morlet, J. 1985 In *Mathematics and physics. Lecture on recent results* (ed. L. Streit), p. 135. Singapore: World Scientific.

Kailasnath, P., Sreenivasan, K., & Stolovitzky, G. 1992 *Phys. Rev. Lett.* **68**, 2766.
Kida, S. 1990 *J. Phys. Soc. Jap.* **60**, 5.
Kolmogorov, A. 1941 *C.R. Acad. Sci. USSR* **30**, 301.
Kolmogorov, A. 1962 *J. Fluid Mech.* **13**, 82.
Leveque, E. & She, Z. 1995 *Phys. Rev. Lett.* **75**, 2690.
Leveque, E. & She, Z. 1997 *Phys. Rev.* E **55**, 2789.
Mallat, S. & Hwang, W. 1992 *IEEE Trans. Inform. Theory* **38**, 617.
Meneveau, C. & Sreenivasan, K. 1991 *J. Fluid. Mech.* **224**, 429.
Meyer, Y. 1990 *Ondelettes*. Paris: Hermann.
Monin, A. & Yaglom, A. 1975 *Statistical fluid mechanics*, vol. 2. MIT Press.
Morel-Bailly, F., Chauve, M., Liandrat, J. & Tchamitchian, P. 1991 *C.R. Acad. Sci. Paris* II **313**, 591.
Muzy, J., Bacry, E. & Arneodo, A. 1991 *Phys. Rev. Lett.* **67**, 3515.
Muzy, J., Bacry, E. & Arneodo, A. 1993 *Phys. Rev.* E **47**, 875.
Muzy, J., Bacry, E. & Arneodo, A. 1994 *Int. Jl Bifur. Chaos* **4**, 245.
Naert, A., Puech, L., Chabaud, B., Peinke, J., Castaing, B. & Hebral, B. 1994 *J. Physique* II **4**, 215.
Neil, O. & Meneveau, C. 1993 *Phys. Fluids* A **5**, 158.
Novikov, E. 1990 *Phys. Fluids* A **2**, 814.
Novikov, E. 1995 *Phys. Rev.* E **50**, 3303.
Obukhov, A. 1962 *J. Fluid Mech.* **13**, 77.
Parisi, G. & Frisch, U. 1985 In *Turbulence and predictability in geophysical fluid dynamics and climate dynamics* (ed. M. Ghil, R. Benzi & G. Parisi), p. 84. Amsterdam: North-Holland.
Pedrizetti, G., Novikov, E. & Praskovsky, A. 1996 *Phys. Rev.* E **53**, 475.
Richardson, L. 1926 *Proc. R. Soc. Lond.* A **110**, 709.
Roux, S. 1996 PhD thesis, University of Aix-Marseille II.
Ruiz-Chavarria, G., Baudet, C. & Ciliberto, S. 1995 *Phys. Rev. Lett.* **74**, 1986.
Schertzer, D. & Levejoy, S. 1987 *J. Geophys. Res.* **92**, 9693.
She, Z. & Leveque, E. 1994 *Phys. Rev. Lett.* **72**, 336.
She, Z. & Waymire, E. 1995 *Phys. Rev. Lett.* **74**, 262.
Siebesma, A. 1988 In *Universality in condensed matter physics* (ed. R. Julien, L. Peliti, R. Rammal & N. Boccara), p. 188. Heidelberg: Springer.
Tabeling, P. & Cardoso, O. (eds) 1995 *Turbulence: a tentative dictionary*. New York: Plenum.
Tabeling, P., Zocchi, G., Belin, F., Maurer, J. & Willaime, H. 1996 *Phys. Rev.* E **53**, 1613.
Vincent, A. & Meneguzzi, M. 1995 *J. Fluid Mech.* **225**, 1.